sustainability

MDPI

Article

Innovative Hybrid Condensing Radiant System for Industrial Heating: An Energy and Economic Analysis

Marco Noro [1,*], Simone Mancin [1], Filippo Busato [2] and Francesco Cerboni [3]

[1] Department of Management and Engineering, University of Padua, 36100 Vicenza, Italy
[2] Economy Department, Università Mercatorum, 00186 Rome, Italy
[3] Officine Termotecniche Fraccaro srl, 31033 Castelfranco Veneto, Italy
* Correspondence: marco.noro@unipd.it; Tel.: +39-0444998704

Abstract: In this paper, an innovative hybrid condensing radiant tubes heating system for an industrial building is modelled in three climatic zones of Italy using dynamic simulation software. Radiant tubes are coupled with an air–water heat pump, the latter serving an air heating system with terminals located in the building. The energy performance of the hybrid heating system is optimized by evaluating the best nominal power of the heat pump, the cut-off temperature in a bivalent parallel operation, the bivalent temperature in a bivalent alternative operation, and the peak power of the photovoltaic system on the roof of the building. Energy savings between 40% and 80% are calculated with respect to traditional heating systems, considering the different configurations of the system and the climates. An economic analysis also allows the evaluation of the economic advantages of this hybrid heating system for industrial buildings.

Keywords: heat pump; heating; hybrid heating system; industrial heating; industry; radiant tube

Citation: Noro, M.; Mancin, S.; Busato, F.; Cerboni, F. Innovative Hybrid Condensing Radiant System for Industrial Heating: An Energy and Economic Analysis. *Sustainability* **2023**, *15*, 3037. https://doi.org/10.3390/su15043037

Academic Editors: Reza Daneshazarian and Shahrzad Soudian

Received: 11 January 2023
Revised: 1 February 2023
Accepted: 6 February 2023
Published: 7 February 2023

1. Introduction

Firstly, a review of the literature on general use and saving of energy in industry is presented, and successively a review on heating and cooling systems of industrial buildings is carried out. In such a context, the main scope and novelty of this paper is finally reported.

1.1. Review of the Literature on Energy Use and Savings in Industry

The production and use of energy account for more than 75% of the greenhouse gas emissions of the European Union (EU). Decarbonising the energy system is critical to reach the 2030 climate goals (reduction by 55% of CO_2 emissions compared with 1990) and the long-term strategy to achieve carbon neutrality by 2050 [1]. One of the main key principles of the European Green Deal is focusing on prioritising energy efficiency, improving the energy performance of buildings, and increasing the share of renewable sources.

The 2018 Energy Efficiency Directive (EED) [2] also sets the energy efficiency target for 2030 as at least 32.5% (to be achieved collectively throughout the EU). Meeting these goals on the reduction of greenhouse gas emissions, the increase in energy efficiency and the use of renewable energy is particularly challenging in the industrial sector. This is one of the largest energy users (after the transport sector) in most EU member states [3], including Italy [4]. In the past, many studies have been conducted to measure the energy consumption of different industrial sectors and to propose energy-saving solutions. In [5], case studies from the literature, reports from the public and industry, and legislation are presented to analyse research and economic incentive strategies for the clean energy industry in Brazil.

Demand side management (DSM) allows the effective harmonisation of demand and supply in order to increase the renewable energy quota. Two different approaches are presented by Leobner et al. [6] in which the energy management system is integrated through demand response strategies. Paulus and Borggrefe [7] investigated the technical and economic potential of DSM in electricity by energy-intensive industries. In [8], the status of the Croatian cement industry and technologies to reduce CO_2 emissions were analysed, also using CFD analysis.

As an energy-intensive industry, some authors approached the use and saving of energy in the glass and steel sectors through the use of radiant waste heat [9]. They presented the conceptual design of a radiant heat capture device, optimising the view factors and optical properties of the surfaces involved to maximise the amount of heat recovered. More recently, Alshehhi et al. [10] demonstrated the potential of thermal energy storage systems to recover heat from high temperature exhaust fumes from the electric arc furnace in the steel industry. In the past, the authors of the present paper investigated the energy savings opportunities in cast iron foundries, both in service plants [11] and in the production process [12].

In [13], the use of integrated phase change material thermal energy storage (PCM TES) systems was evaluated to recover the thermal waste released in industrial processes, thus reducing CO_2 emissions to produce thermal energy. From this point of view, the authors of the present paper studied the enhancement of TES with PCM embedded in aluminium porous matrices, both theoretically [14] and experimentally [15].

Cogeneration can also be considered a high-efficiency technology for industry. For example, Gambini et al. [16] compared different combined heat and power (CHP) solutions for paper industry processes in terms of energy, environmental and economic performance. Vialetto et al. [17] analysed the retrofitting of the energy generation plant of a paper mill using reversible solid oxide cells, thus increasing efficiency and creating a polygeneration system. The same authors proposed the use of big data analysis to design cogeneration systems in industry that could suit energy demand profiles more efficiently by choosing the correct type of cogeneration technology, the operation strategy, and, if necessary, the size of the energy storages [18,19].

On a different topic, Schützenhofer et al. [20] developed a framework to assess the circular economy potential of the architecture, engineering and construction industries, focusing on demolition buildings and construction waste. They compared the ecological impact with the economic and technical efforts required for recycling and reusing processes, reviewing assessment methods, and comparing the essential parameters of material sustainability, efficiency, environmental impact and end-of-life performance.

1.2. Review of the Literature on the Heating and Cooling of Industrial Buildings

Production facilities require considerable amounts of energy for air conditioning. Increased energy costs, regulations and codes on building energy performance [21], and the adoption of the ISO 50,001 standard on energy management systems by national legislation to promote energy efficiency, lead to increasing interest in reducing primary energy consumption for air conditioning of industrial buildings, especially for heating. Industrial facilities are studied in the case of energy retrofit [22], focusing both on the thermal envelope [23] and on service plants such as heating [24] and ventilation [25]. In [26], an analysis was presented using a dynamic simulation of the energy consumption and thermal conditions of industrial buildings. Passive measures to prevent summer overheating were also analysed [27]. In another study [28], the same authors presented a decision support tool to investigate the life cycle of facade systems. A different modelling approach was proposed by Smolek et al. [29]: they decomposed a production facility into modules (energy system, building, logistics and production. Furthermore, the optimisation of two industrial buildings was carried out using building energy modelling and building information modelling tools [30].

To the best knowledge of the authors, only a few studies have reported on the dynamic simulations of the heating and cooling plants of industrial buildings. Recently, Stamponi et al. [31] described a system characterised by a high-performance building, photovoltaic plant, groundwater heat pump, and high-tech control and monitoring system. Selim et al. [32] investigated the potential energy savings in 20 different industrial sectors, suggesting different energy recommendations for each facility, as well as for heating, ventilation and air conditioning (HVAC) systems.

As a matter of fact, industrial buildings feature specific characteristics compared with other types of buildings: usually they present some equipment on the ceiling or walls such as tubes, bridge cranes, pipes, etc.; and they have large doors (often opened), high heights (7 m or more), scarce thermal insulation, and large floor surfaces with different types of occupation by workers [33]. For these reasons, traditional climatisation plants are not used; instead, high-temperature radiant heating systems and air heating systems are quite common. Regarding air heaters, wall-mounted equipment supplied with hot water, ground- or wall-mounted equipment fuelled with natural gas and controlled mechanical ventilation plants are the most common [33].

High-temperature radiant systems are more recent: radiant tubes (modular systems equipped with small gas burners), electrical radiant equipment, or the more traditional types of panels heated by steam or pressurised water [34,35]. High-temperature radiant systems allow the reduction of the air temperature required for comfort conditions as the heat flux can be addressed toward the zone to be heated [36]. However, a better assessment of comfort conditions and energy performance is still necessary [37]. More recently, increased thermal insulation in new buildings determined some interest in coupling condensing boilers and low-temperature radiant heating floor systems [38].

Recently, the authors of the present paper have studied an innovative condensing radiant tubes (CRT) system by means of dynamic simulations to evaluate energy performance and indoor comfort conditions [39]. In such a system, the exhausts from the tubes were coupled to a condensing heat exchanger to produce hot water that fed wall-mounted air heaters, thus enhancing the thermal efficiency of the radiant tubes. The system allowed us to satisfy the heating load with very interesting primary energy savings that could reach 7% compared with a condensing boiler coupled to a radiant floor, but up to 30% with respect to a traditional air heating system [39]. Moreover, it allowed for better performance in terms of thermal comfort conditions, especially during the first hours of operation in the morning, as in real application the floor area was not fully available due to the presence of production equipment and warehouses. More recently, the same authors presented a further development of this system by coupling an air–water heat pump to produce a hybrid heating system (condensing radiant tubes + heat pump system, CRT+HP) [40]. In this way, an enhancement of renewable energy utilisation was realized. To the best knowledge of the authors, no hybrid heating systems using high-temperature radiant tubes have been previously proposed in the scientific literature. Hot water, produced at a medium temperature (40 °C) by exhaust condensation and by the heat pump, fed a thermal storage, which provided heat to wall-mounted air heaters. The authors found that the primary energy saving was extremely high (from 40% in the coldest climatic zones to more than 80% in the mildest) in the case of contextual investment in PV, and lower but still interesting in the case of no PV installation.

1.3. Scope and Novelty of the Study

As the main novelty of this study, a further development of previous work [40] is presented: the effects of a different control logic of the hybrid configuration (bivalent parallel) on energy performance are reported by dynamic simulations with TRNSYS rel. 17 software, with and without the presence of the PV plant. Additionally, an economic analysis is implemented to evaluate the advantage of the hybrid heating system over the benchmark plants.

The main scope is the optimisation of the hybrid configuration by choosing the nominal thermal power of the heat pump, the external air bivalent temperature or the cut-off temperature (refer to next section), and the peak power of the photovoltaic plant to:

- minimise the annual amount of total non-renewable primary energy consumed by the hybrid plant ($PE_{nren,tot}$). This is given by the sum of the non-renewable primary energy consumed with natural gas by the radiant tubes and the non-renewable quota of the electricity imported from the grid;

- minimise CO_2 specific emissions of the plant (kg_{CO2} per square metre of available area);
- maximise the total annual non-renewable primary energy saving compared with traditional heating systems ($PES_{nren,tot}$);
- maximise the primary energy ratio (*PER*), that is, the ratio between the total annual useful thermal energy produced by the plant and the $PE_{nren,tot}$;
- satisfy the requirement of the minimum value of the renewable quota (*QR*), that is 60% according to Italian Legislative Decree 28/2011 [41], D.M. 26/06/2015 [42], UNI/TS 11300-5 [43] and, more recently, Legislative Decree 199/2021 [44] (implementation of the Renewable Energy Source II Directive). *QR* is the ratio between yearly amounts of primary energy:
    - the denominator is the sum of the total primary energy used (renewable + non-renewable) (total primary energy delivered or produced on site, calculated using conversion factors $f_{p,tot} = f_{p,ren} + f_{p,nren}$ [42] for each energy carrier delivered or produced on site);
    - the numerator is the sum of the renewable primary energy produced on site or delivered, calculated using the conversion factor $f_{p,ren}$ [42] for each energy carrier (electricity from the photovoltaic system, electricity from the grid, natural gas, ambient thermal energy as heat pump evaporator heat source).

The solution that guarantees a fair compromise between the three objectives listed above is considered the best, compared with three benchmark heating systems:

- condensing radiant tubes (CRT) (no hybrid system, i.e., without the heat pump);
- air-heater-based system (Air). A 1600 kW ground air heater is installed with a supply air flow rate and a temperature variable as a function of, respectively, the indoor and outdoor air temperature;
- condensing boiler and radiant floor (condensing radiant floor, CRF). It is a radiant floor (distance between tubes 0.3 m, outer diameter and thickness of tubes 0.02 m and 0.002 m respectively, water flow rate 30 kg h^{-1} m^{-2}) coupled to a condensing boiler plant (nominal thermal power 1600 kW, supply water temperature variable as function of outdoor air).

As a variety of plants are present in real situations for Air and CRF, the thermal efficiency of the generators has been varied in suitable ranges for both Air and CRF in order to represent both new (0.80–0.84 for Air, 0.90–0.96 for CRF) and old plants (0.70–0.72 for Air, 0.87–0.93 for CRF). The latter are indicated as 'Air_old' and 'CRF_old' in next sections.

The structure of the paper is set up by the Materials and Methods section (where the simulation models of the building and the plants are summarised) and the Results and Discussion section (where the simulation results are reported firstly in the presence and then in the absence of the PV plant). For both cases, the bivalent parallel operation is synthesised first, followed by the bivalent alternative one. After some remarks on the annual energy comparison, an economic and sensitivity analysis is also carried out. Finally, some conclusions are reported.

2. Materials and Methods

The study is structured by the following steps:

1. modelling of a typical industrial building whose characteristics are based on a real case to calculate the annual heating load in three different climates;
2. modelling of the hybrid CRT+HP system and analysis of the energy performance. The main scope of this step is to find, for each climate, the best set of:
    - useful thermal power of the HP (P_{th_HP});
    - bivalent temperature in alternative bivalent operation (T_{biv}). In this case, the heat pump has priority; when the external temperature is below the "bivalent" value, the radiant tubes are turned on and the heat pump is switched off;

- cut-off temperature in parallel bivalent operation ($T_{cut\text{-}off}$), that is, the heat pump remains in operation even with external air below the bivalent temperature and until a further threshold, the "cut-off" temperature, in parallel with the radiant tubes;
- peak power of the PV field (P_{PV}).

3. modelling of the three benchmark heating systems as described above to be compared with the CRT+HP hybrid system. The comparison is carried out from both an energy and economic point of view.

2.1. Industrial Building Modelling

The energy performances of the four systems are evaluated in a real industrial building whose characteristics in terms of size and thermal properties of opaque and transparent structures of the two thermal zones are described in the previous work [40], and here reported in Tables 1 and 2. The three resorts considered are in very different climatic zones following the Italian DPR 412/93 [45], increasing the number of degree days (DD) (and therefore the heating needs of the building) from zone D (1415 DD) to zone E (2814 DD) to zone F (3376 DD) [46]. The authors concentrated on the three coldest climatic zones in Italy (zones D-E-F) because they represent the greatest part of national natural gas consumption for building heating, more than 90% [47].

Table 1. Thermal transmittance of opaque and transparent structures of thermal zones of the building.

Parameter (Unit)	Value
Thermal transmittance (W m^{-2} K^{-1})	
External wall	0.389
Door	3.50
Main door	3.50
Wall-facing offices	2.954
Base-facing wall	3.220
Floor-facing ground	0.128
Ceiling	4.086
Ceiling shed	0.208
Window	5.0
Thermal bridge wall–floor facing ground (W m^{-2} K^{-1})	0.353
Thermal bridge wall–ceiling (W m^{-2} K^{-1})	0.262

Table 2. Main characteristics of the two thermal zones of the building for TRNSYS simulation.

	Thermal Zone 1	Thermal Zone 2
Floor area (m^2)	7119	716.5
Net height (m)	8.24	8.22
Indoor air temp. (°C)	18	18
Net volume (m^3)	58,669	5886.2
Heating scheduling	6.00 am to 6.00 pm	6.00 am to 6.00 pm
Heat gain for people and lighting (W m^{-2})	5	5
People and lighting scheduling	8.00 am to 6.00 pm	8.00 am to 6.00 pm
Presence of people	40	8
Degree of activity (met)	2 met	2 met
Clothing (clo)	1 clo	1 clo
Air infiltration (vol h^{-1})	0.5	0.5

The heating needs on a daily basis are reported in Figure 1 as a result of the dynamic simulation (0.25 h time step, the weather data were obtained by interpolation from hourly values in [46]). Based on the real installed power of the condensing radiant tubes (1200 kW, 1500 kW and 1500 kW for the climatic zone D, E, and F, respectively), the thermal power of the heating generators has been limited to such values.

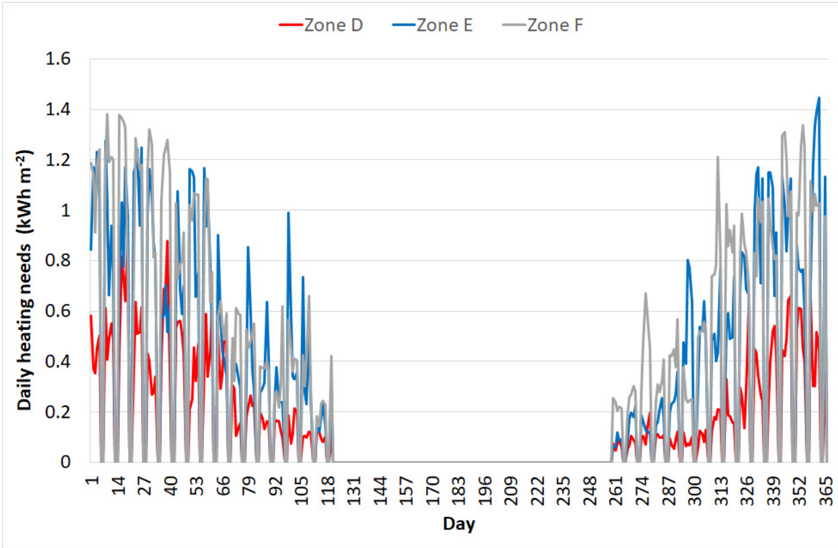

Figure 1. Thermal energy in specific terms for daily heating needs for the three thermal zones. It is the sum of sensible heating and infiltration of outdoor air.

2.2. Heating Systems Modelling

The CRT is an innovative system proposed by an Italian manufacturer based on a radiant tubes system whose exhausts are directed to a condensing heat exchanger to produce hot water (at around 40–50 °C). In the hybrid configuration proposed here (CRT+HP), an air–water heat pump is coupled to limit the operation of radiant tubes and increase the renewable energy utilisation. Hot water at 40 °C produced by the heat pump and the condensing heat exchanger feeds the wall-mounted air heaters by means of a suitable thermal energy storage (here is supposed to be 1000 L) (Figure 2). The CRT system is simulated in TRNSYS by coupling types 607 and 659, suitably modified to simulate the operation of the high temperature radiant tube system. The CRT burner is turned on at maximum power to obtain the maximum exhausted temperature. With increasing of the indoor air temperature, the set point is approached, and the thermal power of the CRT burner is modulated by the proportional valve of natural gas. Fuel modulation decreases the exhausted temperature, and the exhausted tab is regulated to have the correct minimum air excess in the burner.

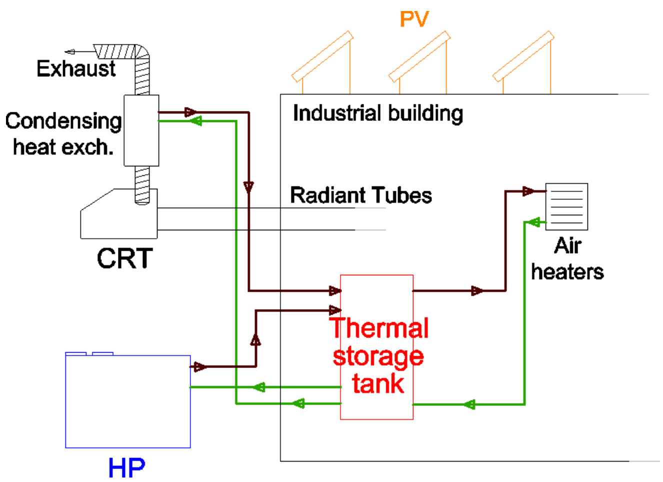

Figure 2. Simplified functional diagram of the CRT+HP plant. The HP and the condensing heat exchanger feed the thermal storage tank to supply hot water at 40 °C to the air heaters (installed on the walls of the building). The condensing radiant tubes (installed on the ceiling of the building) provide heating by means of radiation and convection.

The nominal data of the heat pump, simulated by means of type 941, are reported in Table 3. More details concerning the TRNSYS simulation models of the hybrid (Figure 3) and the reference systems are reported in references [39,40].

Table 3. Nominal data of the air–water heat pump (D.B. = dry bulb temperature; W.B. = wet bulb temperature).

T_{ext} (°C)		$T_{out,cond}$ (°C)					
D.B.	**W.B.**	**35**			**40**		
		kW_{th}	kW_{el}	COP	kW_{th}	kW_{el}	COP
−7	−8	205.0	60.8	3.37	203.0	67.8	2.99
−5	−6	216.0	61.2	3.53	214.0	68.0	3.15
0	−1	245.0	62.4	3.93	243.0	68.9	3.53
2	1	260.0	62.8	4.14	256.0	69.4	3.69
7	6	297.0	64.1	4.63	290.0	70.7	4.10
12	11	344.0	65.7	5.24	336.0	72.1	4.66

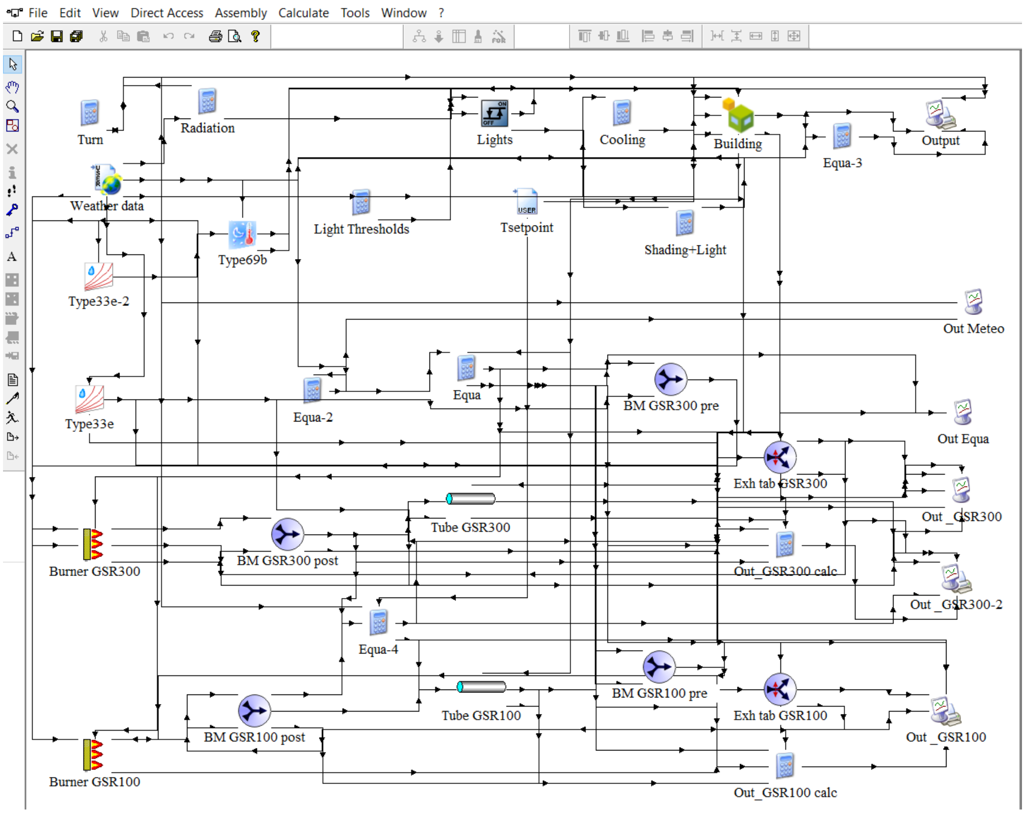

Figure 3. TRNSYS project of building and hybrid condensing radiant tubes heating plant.

The control logic of the system provides, for each time step, the priority operation of the heat pump that produces the thermal power (at the outlet of the condenser $T_{out,cond}$ = 40 °C) according to the external air temperature (T_{ext}). Two modes of operation of the heat pump are considered:

- alternative bivalent mode: HP shutdown is when $T_{ext} < T_{biv}$ (bivalent temperature T_{biv} has to be optimised);
- parallel bivalent mode: HP shutdown occurs when $T_{ext} < T_{cut\text{-}off} < T_{biv}$ with parallel operation of HP and CRT when $T_{cut\text{-}off} < T_{ext} < T_{biv}$ (cut-off temperature $T_{cut\text{-}off}$ has to be optimised).

The quota of the heating load that is not covered by the heat pump is satisfied by the radiant tubes, considering a minimum load factor for the latter equal to 30%. In each time step, thermal storage compensates for any deficit or surplus of thermal energy produced by the generators.

The analysis was carried out both with and without the presence of a photovoltaic field. The electricity produced can cover (totally or partially) the consumption of the heat pump. The peak power of PV is optimized by simulations. Table 4 shows the values of the main parameters used in the energy and economic analysis, whose results are reported in the next section. The interest rate of 2.0% is considered as a 'real' interest rate, calculated on a suitable monetary interest rate (which depends on many variables and can be fixed, for a renewable energy project, at 12%) and the actual inflation rate (around 10% in Italy at the period of writing).

Table 4. Main parameters for energy and economic analysis.

Symbol	Meaning	Value
$f_{p,nren,NG}$	Non-renewable primary energy conversion factor for natural gas [42]	1.05
$f_{p,nren,el}$	As above for electricity from the grid [42]	1.95
$f_{p,ren,el}$	Renewable primary energy conversion factor for electricity from the grid [42]	0.47
$f_{p,ren,PV}$	As above for electricity from the PV field [42]	1
$f_{p,ren,heat\_source\_HP}$	As above for external air thermal energy [42]	1
QR	Minimum renewable ratio for new buildings [42]	60%
PV [kW_p]	(Reference) peak power	200
PV [η_{nom}]	(Reference) peak efficiency	16.0%
PV [m^2 kW_p^{-1}]	(Reference) specific area	6.3
Emiss. CO_2 [kg_{CO2} kWh^{-1}]	Specific CO_2 emission factor	
Electricity from the grid		0.4
Natural gas (NG)		0.2
NG cost [€ Sm^{-3}]	-	1.00
Electricity from the grid cost [€ kWh^{-1}]	-	0.20
Electricity exported value [€ kWh^{-1}]	-	0.10
CRT+HP investment cost [€] **	-	300,000
PV investment cost [€ W_p^{-1}] [48]	-	1.0
Interest rate/Period of the analysis [y]	-	2.0%/15

** Based on the experience of the authors and the industrial partner that built the radiant tubes.

3. Results and Discussion

For the three climatic zones D, E and F, a sensitivity analysis referring to the energy performance of the hybrid CRT+HP heating system is presented. This analysis allows us to find the best energy performance configuration of the hybrid system. Furthermore, for the optimised set-up of the CRT+HP plant, non-renewable primary energy savings ($PES_{nren,tot}$) are reported for the different cases analysed with respect to the benchmark heating systems. Finally, an economic evaluation of the proposed hybrid system is provided.

3.1. Energy Analysis with Photovoltaic Power

3.1.1. Bivalent Parallel Operation

The sensitivity analysis for this configuration is reported in Figures 4–6. The main indices (PER, $PE_{nren,tot}$, QR, CO_2 specific emission) are reported on the y-axis, varying (in the x-axis) the cut-off external air temperature ($T_{cut\text{-}off}$), the peak power of the photovoltaic system (P_{PV}), and the nominal power of the heat pump (P_{th_HP}). Based on the reference values in Table 4, the sensitivity analysis allows us to find the best values of these four variables. A similar analysis has been developed for all the considered cases (with and without PV, parallel and alternative operation). As depicted in Figures 4–6, for parallel operation with the PV plant the most advantageous configuration is established in the climatic zones D, E and F, respectively (T_{biv} = 5 °C): $T_{cut\text{-}off}$ = −2.5 °C, −5 °C, −5 °C; thermal power of the heat pump (P_{th_HP}) = 493 kW_{th} (170% of the nominal data, 41% of the installed power of the radiant tubes), 580 kW_{th} (200% of the nominal output, 38% of the nominal power of the radiant tubes), and 493 kW_{th} (170% of the nominal output, 33% of the installed power of the radiant tubes); and peak power of the photovoltaic system (P_{PV}) = 340 kW_p (170% of the nominal data in Table 4 for all climatic zones).

Climatic zone D

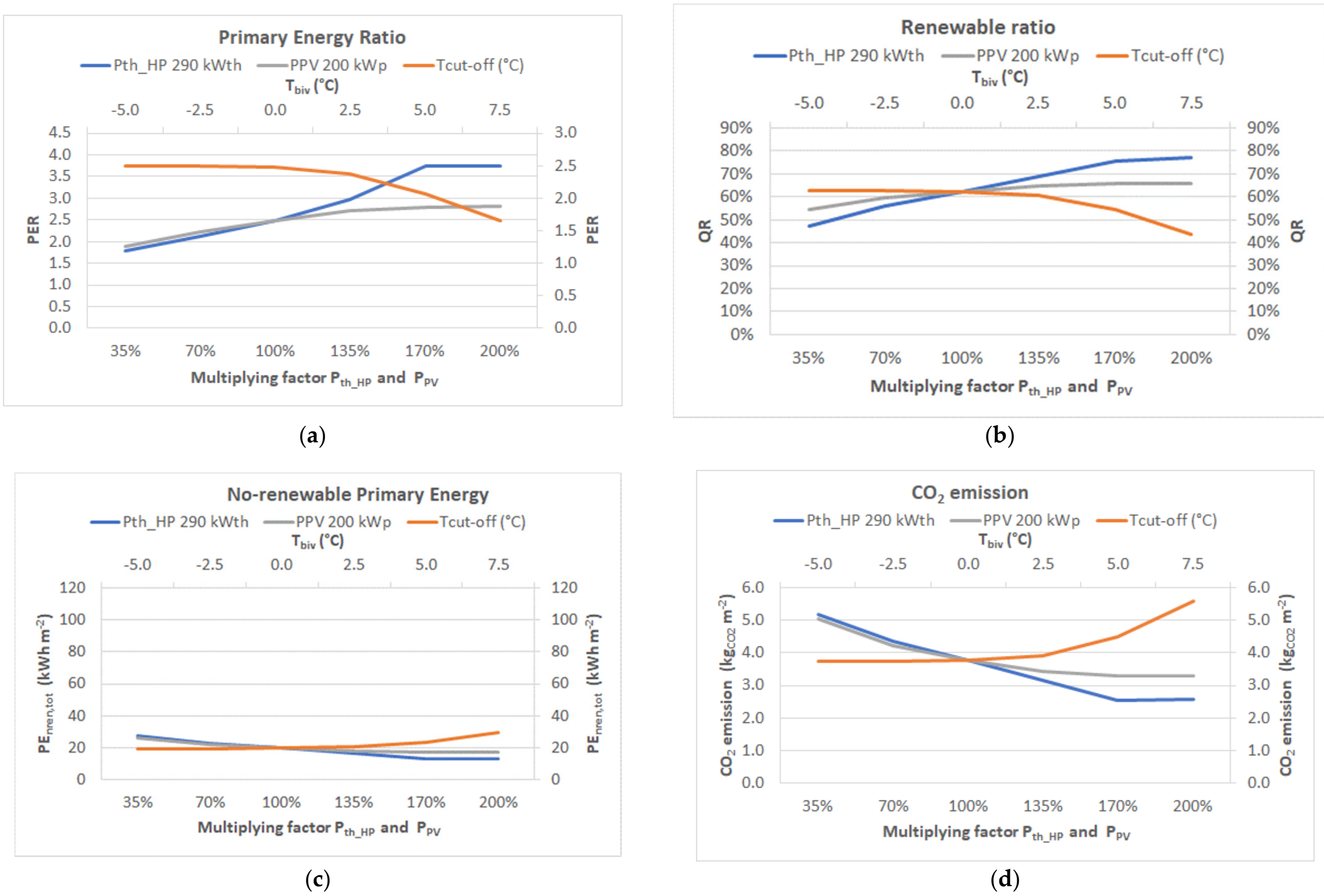

Figure 4. *PER* (**a**), *QR* (**b**), $PE_{nren,tot}$ (**c**) and specific CO_2 emission (**d**) varying the multiplying factor of the nominal output of the heat pump (P_{th_HP}) and the peak power of the photovoltaic system (P_{PV}) (lower abscissa) and varying the cut-off temperature (upper abscissa) (with PV, bivalent parallel operation), for the climatic zone D.

Comparing parts (a) of Figures 4–6, the *PER* in colder climates is lower than in climatic zone D. This is due to the lower utilisation of renewable energy by the heat pump because of the lower *COP* and the lower electricity production of the PV plant. This extends the use of radiant tubes (i.e., natural gas). However, this decrease is lower than in the case of the bivalent alternative operation (see Section 3.1.2). Climate zones E and F benefit more from the parallel bivalent operation. Consequently, *QR* exceeds the value of 60% not only in climatic zone D but also in zone E (Table 5).

Climatic zone E

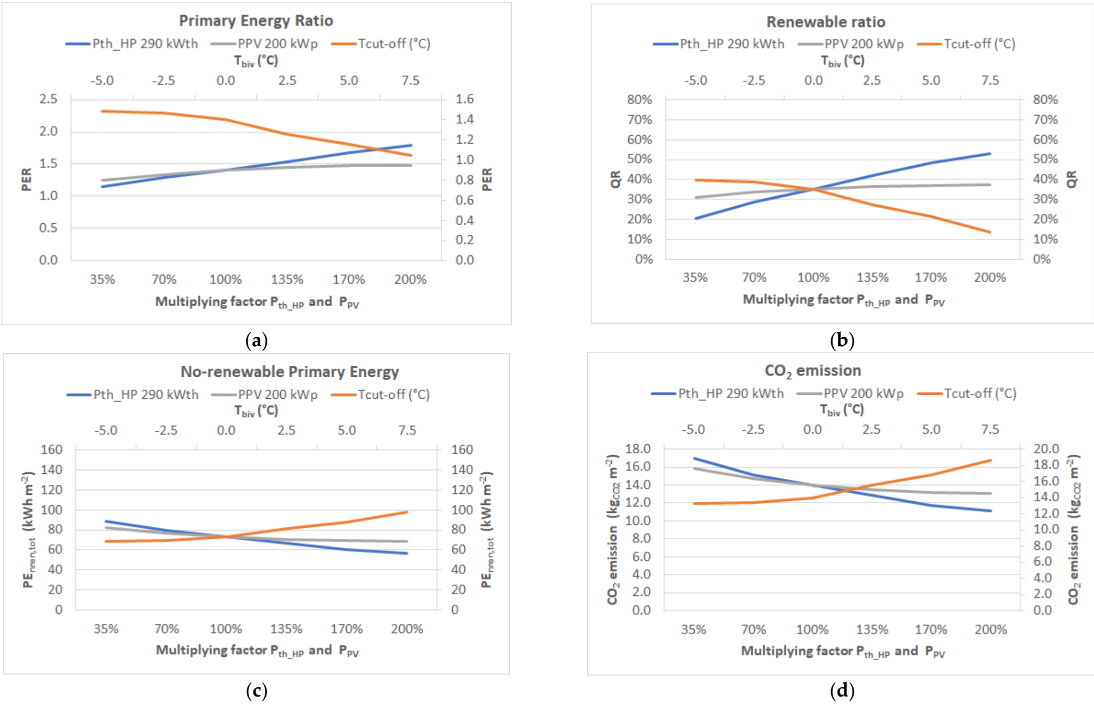

Figure 5. *PER* (**a**), *QR* (**b**), $PE_{nren,tot}$ (**c**) and specific CO_2 emission (**d**) varying the multiplying factor of the nominal output of the heat pump (P_{th_HP}) and the peak power of the photovoltaic system (P_{PV}) (lower abscissa) and varying the cut-off temperature (upper abscissa) (with PV, bivalent parallel operation), for the climatic zone E.

Climatic zone F

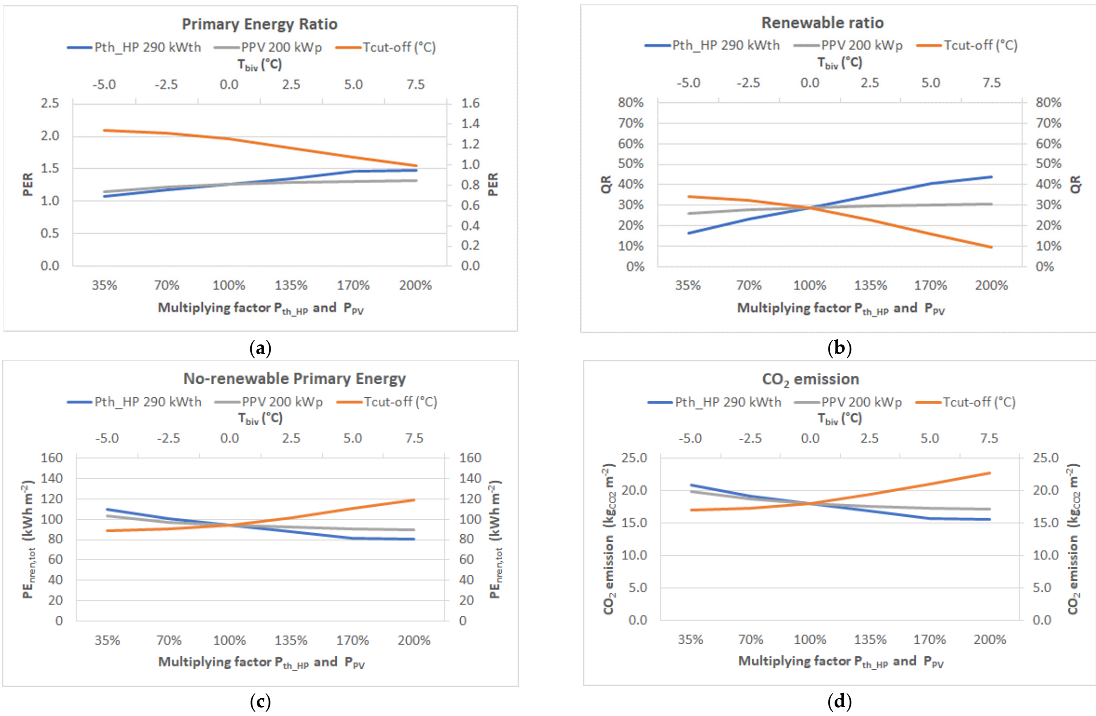

Figure 6. *PER* (**a**), *QR* (**b**), $PE_{nren,tot}$ (**c**) and specific CO_2 emission (**d**) varying the multiplying factor of the nominal output of the heat pump (P_{th_HP}) and the peak power of the photovoltaic system (P_{PV}) (lower abscissa) and varying the cut-off temperature (upper abscissa) (with PV, bivalent parallel operation), for the climatic zone F.

Table 5. Energy performance indices of the CRT+HP system in the optimal configuration for the three climatic zones (annual values) (*PE*=primary energy) (with PV, bivalent parallel operation).

Symbol	Description	Unit	Zone D	Zone E	Zone F
$PE_{ren,el}$	Renewable quota of electricity from the grid	[kWh]	3272	28,764	29,170
$PE_{nren,el}$	Non-renewable quota of electricity from the grid	[kWh]	13,575	119,339	121,026
$PE_{ren,PV}$	Renewable quota of electricity from the PV self-consumed	[kWh]	77,500	120,191	107,408
$PE_{ren,PV,exp}$	Renewable quota of electricity from the PV exp. to grid	[kWh]	431,186	346,681	266,584
$PE_{ren,heat\_source\_HP}$	Thermal energy as heat source of the HP	[kWh]	246,431	452,206	415,447
$PE_{ren,tot}$	Total renewable	[kWh]	327,203	601,160	552,026
$PE_{nren,NG}$	Non-renewable as natural gas	[kWh]	55,464	195,911	390,089
$PE_{nren,tot}$	Total non-renewable	[kWh]	69,040	315,250	511,115
PER	Primary energy ratio		5.51	2.54	1.82
QR	Renewable ratio		82.6%	65.6%	51.9%
$PE_{nren,tot}$	Specific total non-renewable	[kWh m^{-2}]	8.8	40.2	65.2
CO_2		[kg$_{CO2}$ m^{-2}]	1.7	7.9	12.7

The hybrid system allows extremely high savings of non-renewable primary energy compared with all other solutions, especially in milder climates (zone D) (Figure 7). Very high $PES_{nren,tot}$ of the hybrid CRT+HP plant have been calculated even if considering the condensing radiant tube plant (CRT), which the same authors revealed to be an efficient solution [39].

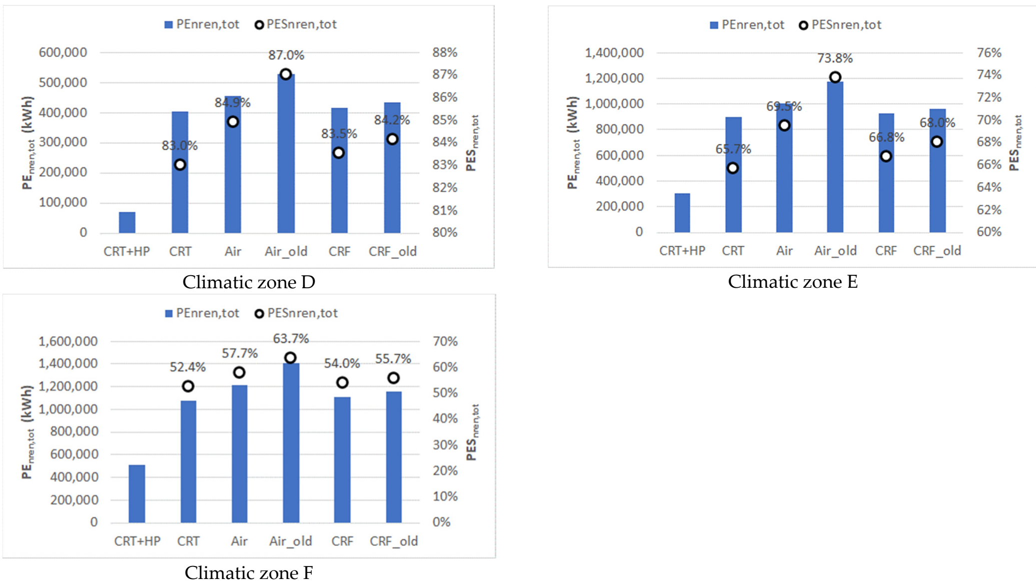

Figure 7. Total annual non-renewable primary energy consumption ($PE_{nren,tot}$) and savings of the same energy ($PES_{nren,tot}$) of the hybrid CRT+HP system in the optimal configuration (with photovoltaic, bivalent parallel operation).

3.1.2. Bivalent Alternative Operation

This configuration was already studied in [40], and the main results are synthesised here. Regarding the climatic zones D, E, and F, the results for the best configuration are, respectively: P_{th_HP} = 493–392–392 kW$_{th}$ (170–135–135% of the nominal data, which is 41–25–25% of the thermal power of the radiant tubes (1200–1500–1500 kW$_{th}$)); T_{biv} = 0–0–0 °C; P_{PV} = 340–270–270 kW$_p$ (170–135–135% of the data in Table 4).

As reported in [40], in colder climates, the *PER* and *QR* of the CRT+HP system in the optimal configuration decrease because the heat pump uses a minor amount of renewable energy, thus extending the use of radiant tubes. In fact, the lower *COP* and the lower electricity production of the PV plant reduce the renewable energy quota used by the heat pump. Only in climatic zone D is it possible to exceed the value of 60% for *QR*. The annual value of the *PER* is quite high in general, and extremely high in milder climates.

As a consequence, the hybrid CRT+HP system features very high non-renewable primary energy savings, especially in milder climates (zone D) due to the greater contribution of renewable sources (electricity from photovoltaics and thermal energy from the ambient air to the evaporator) in input to the heat pump (Figure 8). However, in more rigid climatic zones, the parallel operation described in previous Section 3.1.1 allows for a considerable increase in the $PES_{nren,tot}$ with respect to the alternative operation: in zone E the $PES_{nren,tot}$ increases by about 15 percentage points compared with the Air system, and somewhat more compared with the CRF system (Figure 7 vs. Figure 8b).

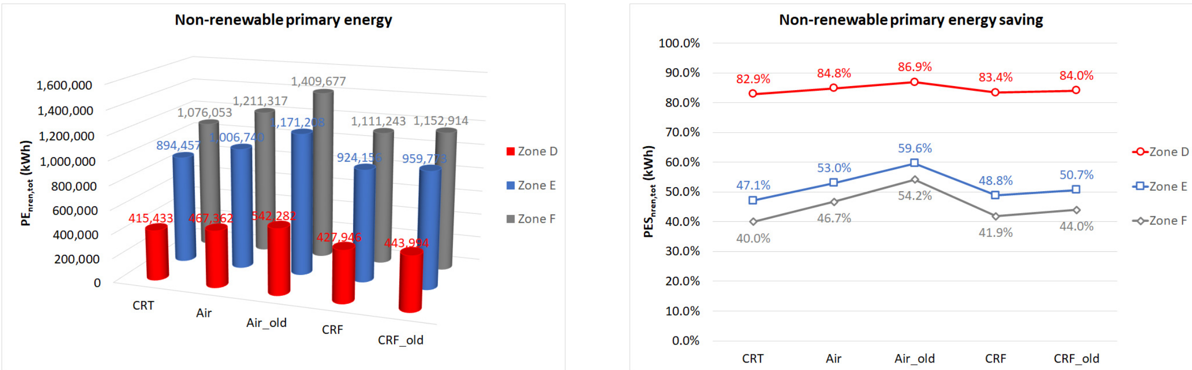

(**a**) (**b**)

Figure 8. $PE_{nren,tot}$ (**a**) and $PES_{nren,tot}$ (**b**) in the optimal configuration of the hybrid CRT+HP system (with photovoltaic bivalent alternative operation).

3.2. Energy Analysis without PV

3.2.1. Bivalent Parallel Operation

Unlike the following alternative operation mode, in this case the optimal thermal power of the heat pump that optimises energy performance (P_{th_HP}) does not decrease from the climatic zone D to F: it is always 200% of the nominal value (that is, 580 kW_{th}, 48%, 39% and 39% of the installed power of the radiant tubes in zones D, E and F, respectively) (Figure 9) (with T_{biv} = 5 °C and $T_{cut\text{-}off}$ = −2.5 °C). Even though the $PES_{nren,tot}$ is lower than the case with the PV plant, it is still high, especially in milder climates (in zone D $PES_{nren,tot}$ is equal to 44% with respect to the CRT and 58% with respect to the 'Air_old' system).

3.2.2. Bivalent Alternative Operation

As reported in [40], from the climatic zone D to F, the nominal thermal power of the heat pump that optimises energy performance (P_{th_HP}) decreases. In fact, in zones D and E it is 200% of the nominal value (that is, 580 kW_{th}, 48% and 39% of the nominal installed power of the radiant tubes, respectively), while in zone F it is 170% (that is, 493 kW_{th}, 33% of the nominal installed power of the radiant tubes) (considering T_{biv} = 5 °C). Moreover, the hybrid system allows for high $PES_{nren,tot}$ (even if they are lower than in the case with PV) thanks to the high contribution of renewables at the HP evaporator, especially in milder climates (in zone D, $PES_{nren,tot}$ is equal to 30% with respect to the CRT and 47% with respect to the 'Air_old' system).

3.3. Remarks on the Energy Performance of the Hybrid System

As previously stated, the hybrid system allows for very high *PER*, especially in milder climates: in zone D with the photovoltaic field, it exceeds the value of five. In colder climates, the lower use of renewable energy by the HP (both the electricity produced by the PV plant and the thermal energy available at the evaporator) implies a decrease in *PER*. The climatic zones E and F benefit more from the parallel bivalent operation since the decrease in *PER* with respect to zone D is lower (Table 6). *QR* decreases substantially in colder climates for the same reasons, and the value of 60% is exceeded only with photovoltaic energy. The parallel bivalent operation allows this threshold to be exceeded not only in zone D but also in zone E (Table 6).

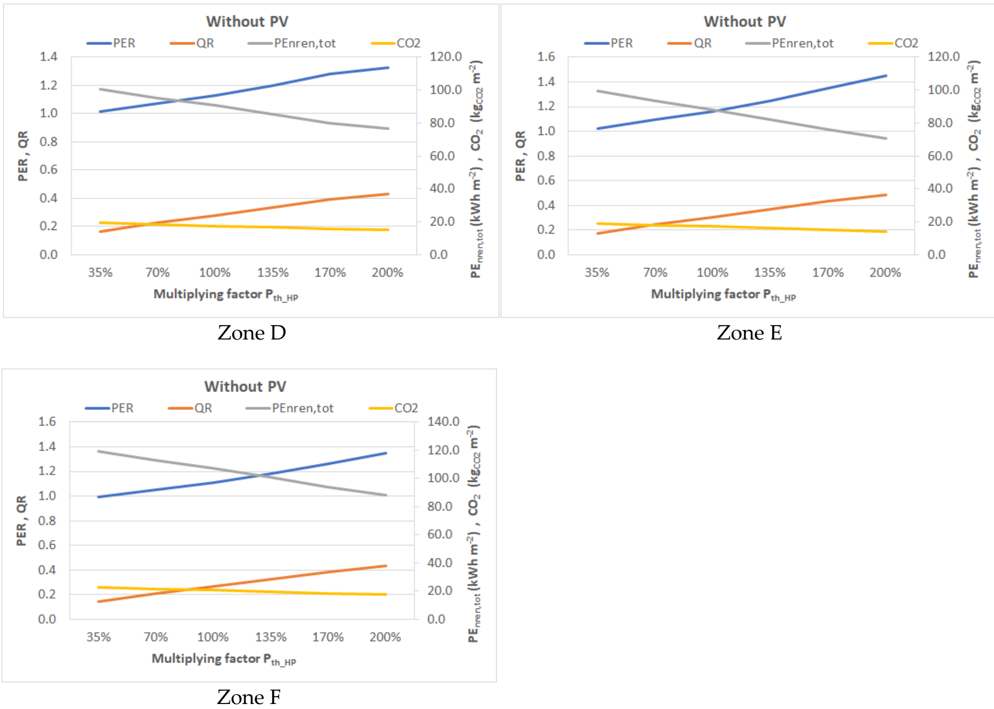

Figure 9. $PE_{nren,tot}$, *PER*, *QR*, and specific CO_2 emission varying the P_{th_HP} multiplying factor (without PV, bivalent parallel operation).

Table 6. Energy performance of the CRT+HP system in optimal configuration in the various cases.

			Zone D	Zone E	Zone F
PV–ALTERNATIVE	*PER*		5.35	1.69	1.44
	QR		82.2%	45.3%	37.0%
	$PE_{nren,tot}$	[kWh m^{-2}]	9.1	60.4	82.4
	CO_2	[kg_{CO2} m^{-2}]	1.8	11.5	15.8
PV–PARALLEL	*PER*		5.51	2.54	1.82
	QR		82.6%	65.6%	51.9%
	$PE_{nren,tot}$	[kWh m^{-2}]	8.8	40.2	65.2
	CO_2	[kg_{CO2} m^{-2}]	1.7	7.9	12.7
NO PV–ALTERNATIVE	*PER*		1.73	1.33	1.21
	QR		56.5%	43.2%	37.1%
	$PE_{nren,tot}$	[kWh m^{-2}]	28.1	76.9	98.5
	CO_2	[kg_{CO2} m^{-2}]	5.7	15.2	19.3
NO PV–PARALLEL	*PER*		1.73	1.45	1.35
	QR		56.6%	48.5%	43.5%
	$PE_{nren,tot}$	[kWh m^{-2}]	28.0	70.5	88.3
	CO_2	[kg_{CO2} m^{-2}]	5.6	14.1	17.5

3.4. Economic Analysis

Table 7 reports the main results in terms of net present worth (*NPW*) and discounted payback period (*DPP*). These indices were calculated on the basis of the interest rate value and the economic analysis period shown in Table 4. The reported CAPital EXPenditures (CAPEX) were provided by the experience of the authors.

Table 7. Annual investment (CAPEX), operating costs (OPEX) and net present worth (*NPW*) of the different plants; discounted payback period (*DPP*) of the hybrid CRT + HP system in the optimal configuration compared with other systems. Negative values indicate an expenditure, and positive values indicate an income. The values of the benchmark systems are reported in the first case only.

		Zone D				**Zone E**				**Zone F**			
		CAPEX [€]	**OPEX [€]**	***NPW* [€]**	***DPP* [y]**	**CAPEX [€]**	**OPEX [€]**	***NPW* [€]**	***DPP* [y]**	**CAPEX [€]**	**OPEX [€]**	***NPW* [€]**	***DPP* [y]**
PV–BIV. ALT.	CRT+HP	−640,000	36,521	−170,736	-	−640,000	−6,439	−722,732	-	−640,000	−30,548	−1,032,515	-
	CRT	−200,000	−36,557	−669,732	6.5	−200,000	−81,238	−1,243,850	6.3	−200,000	−97,486	−1,452,620	7.1
	Air	−150,000	−41,143	−678,655	6.8	−150,000	−91,429	−1,324,790	6.2	−150,000	−109,714	−1,559,748	6.7
	Air_old	−120,000	−47,871	−735,113	6.6	−120,000	−106,381	−1,486,917	5.5	−120,000	−127,657	−1,760,300	5.7
	CRF	−200,000	−37,757	−685,151	6.4	−200,000	−83,905	−1,278,114	6.1	−200,000	−100,686	−1,493,737	6.8
	CRF_old	−170,000	−39,214	−673,875	6.7	−170,000	−87,143	−1,289,722	6.3	−170,000	−104,571	−1,513,666	6.9
PV–BIV. PAR.	CRT+HP	−640,000	36,696	−168,490	-	−640,000	4659	−580,141	-	−640,000	−21,137	−911,592	-
	CRT				6.5				5.5				6.2
	Air				6.8				5.4				5.9
	Air_old				6.6				5				5.2
	CRF				6.4				5.3				5.9
	CRF_old				6.7				5.5				6
NO PV–BIV. ALT.	CRT+HP	−300,000	−27,109	−648,331	-	−300,000	−71,771	−1,222,198	-	−300,000	−86,201	−1,407,615	-
	CRT				12				12				9.9
	Air				12.1				8.4				6.9
	Air_old				9.6				5.5				4.6
	CRF				10.5				9.1				7.5
	CRF_old				12.2				9.4				7.7
NO PV–BIV. PAR.	CRT+HP	−300,000	−22,442	−588,360	-	−300,000	−53,959	−993,338	-	−300,000	−66,956	−1,160,341	-
	CRT				7.7				3.8				3.4
	Air				8.8				4.2				3.7
	Air_old				7.7				3.6				3.1
	CRF				7.1				3.5				3.1
	CRF_old				8.5				4.1				3.6

With the presence of the photovoltaic plant, the bivalent alternative operation features a more advantageous investment in terms of the payback time of the CRT+HP hybrid solution in climatic zone E than in milder climates (zone D) compared with other systems, especially with regard to air systems. In terms of *NPW*, the hybrid solution appears to be more advantageous in zone D, as it allows for both lower CAPEX and lower OPerational EXPenditures (OPEX).

Even in the case of parallel operations, the investment in the hybrid solution CRT+HP reveals to be more advantageous in terms of *DPP* in rigid climates (climatic zones E and F) than in milder climates (zone D) compared with the other solutions. With respect to alternative operations, a reduction of *DPP* is appreciable only in cold climates (zones E, F), while in zone D there are no substantial differences. However, in zones E and F, there is an appreciable increase in *NPW* compared with the alternative operation.

In the absence of the photovoltaic system, the greater convenience of the investment in terms of a shorter payback time in colder climates is more pronounced in both alternative and parallel operations. Furthermore, the latter operation mode allows for a lower *DPP* than the alternative bivalent operation because of the more extended use of the heat pump.

The results in Table 7 confirm the correctness of considering only colder climatic zones of Italy (D, E, F). As, in general terms, the economic profitability of the CRT+HP system increases from milder to colder climates, its economic performance would certainly be worse in warmer climates.

3.5. Sensitivity Analysis

To assess how energy prices affect *NPW* and *DPP*, a sensitivity analysis was performed for the case that featured the best energy performance (with photovoltaic system, parallel bivalent operation, climate zone E, with T_{biv} = 5 °C and $T_{cut\text{-}off}$ = −2.5 °C).

The cost of energy was varied in the following ranges:

- natural gas: 0.5–1–1.5 € Sm^{-3} (Figure 10);
- electricity from the grid: 0.15–0.25–0.35 € kWh_{el}^{-1} (Figure 11).

The central values of the proposed triplets are those at the beginning of the war in Ukraine (March 2022), the lowest values refer to the pre-crisis situation (pandemic, cost of raw materials and war in Ukraine), while the highest values refer to the present scenario of increases in the cost of energy.

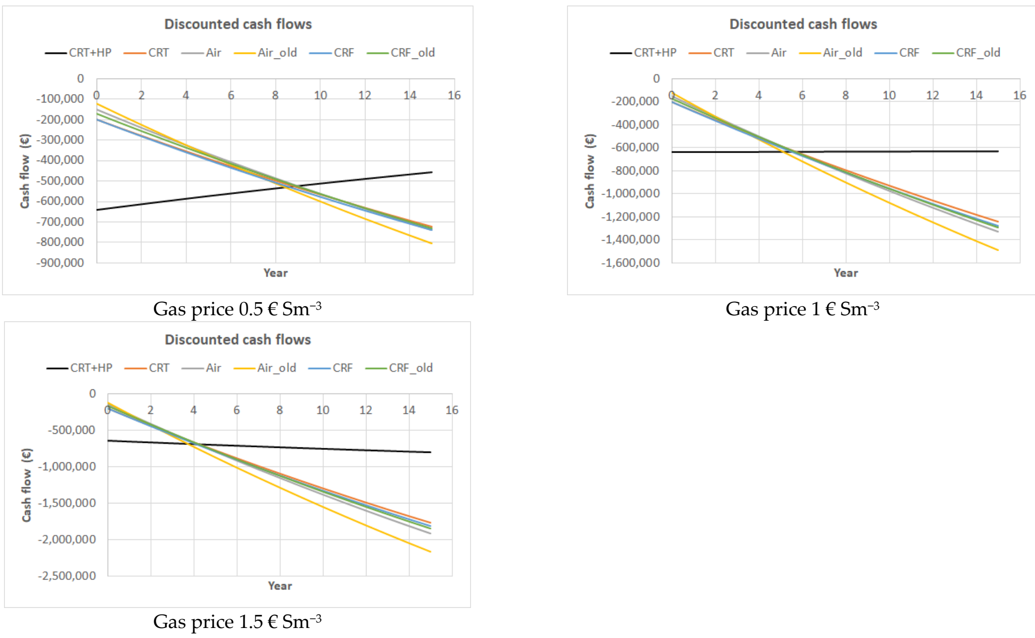

Figure 10. Discounted cash flows of the various systems compared, for climatic zone E, with photovoltaic system, bivalent parallel operation and electricity from the grid price 0.2 € kWh_{el}^{-1}.

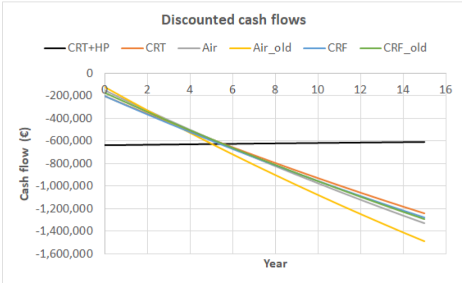

Electricity from the grid price 0.15 € kWh$_{el}^{-1}$

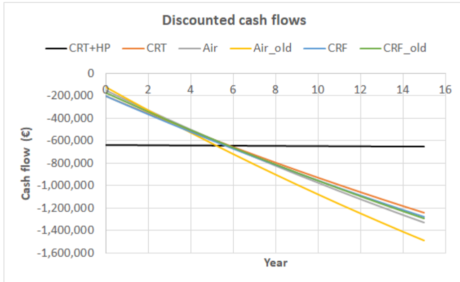

Electricity from the grid price 0.25 € kWh$_{el}^{-1}$

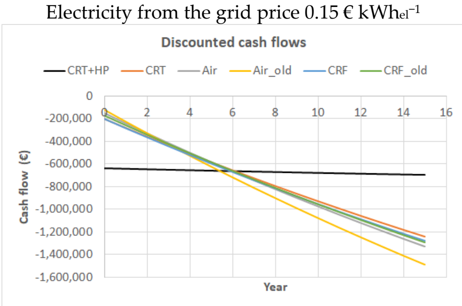

Electricity from the grid price 0.35 € kWh$_{el}^{-1}$

Figure 11. Discounted cash flows of the various systems compared, for climatic zone E, with photovoltaic system, bivalent parallel operation and gas price 1 € Sm^{-3}.

The graphs in Figures 10 and 11 show the trends in discounted cash flows. The values of *NPW* (value of the curves at the end of the economic analysis period, 15 years as reported in Table 4) and *DPP* (abscissa at the intersection of the black curve with the others) can be read. It is apparent that, in the presence of the photovoltaic system, the cost of natural gas affects the increase in *DPP* and the decrease in *NPW* much more than the cost of electricity from the grid. On the contrary, in the absence of the photovoltaic system, the sensitivity of the economic indices to variations in the cost of electricity increases considerably, with *DPPs* that tend to become extremely long and *NPWs* that are very penalising (Figure 12).

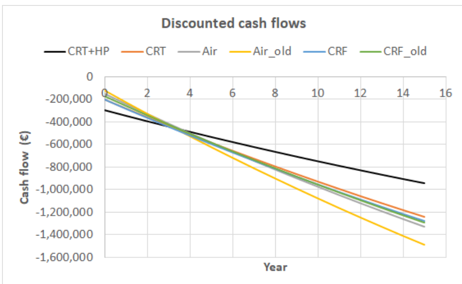

Electricity from the grid price 0.15 € kWh$_{el}^{-1}$

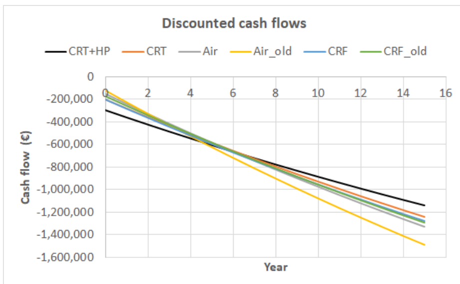

Electricity from the grid price 0.25 € kWh$_{el}^{-1}$

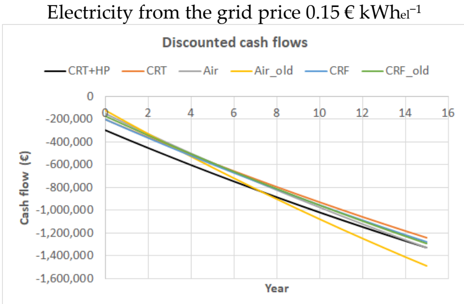

Electricity from the grid price 0.35 € kWh$_{el}^{-1}$

Figure 12. Discounted cash flows of the various systems compared, for climatic zone E, without photovoltaic system, bivalent parallel operation and gas price 1 € Sm^{-3}.

4. Conclusions

In climatic zone D, when a photovoltaic system is installed, it is not convenient to size the heat pump of the hybrid CRT+HP system by more than 40% of the thermal power of the radiant tubes. This percentage is 25% in zones E and F. In colder climates, these percentages may increase in the case of a parallel bivalent operation, reaching 38% and 33%, respectively, in zones E and F.

The most suitable values of bivalent temperature (alternative operation) and cut-off temperature (parallel operation) are equal, respectively, to 0 °C and −2.5 °C in zone D, 0 °C and −5 °C in zone E, 0 °C and −5 °C in zone F. The optimal PV peak power is between 5.5 and 7.5 $m^2\ kW_p{}^{-1}$ in the range of 14–19% for the nominal efficiency) for both the alternative and parallel operation modes.

Very high *PER* of the hybrid CRT+HP system can be performed in the optimised configuration, especially in milder climates (a value greater than five in zone D is reached in the presence of the photovoltaic system). It decreases in the colder zones E and F, even if the parallel bivalent operation is more advantageous from this point of view. The value of 60% for *QR* is exceeded only when installing the photovoltaic system, whereas the parallel bivalent operation allows this threshold to be exceeded, not only in climatic zone D but also in zone E.

In addition, very high primary energy savings are calculated with respect to the reference plants, from 40% (climatic zone F) to values greater than 80% (climatic zone D) in the case of the alternative bivalent operation and in the presence of the photovoltaic system, even better in the case of the parallel bivalent operation (respectively 50% and 80%). Such values are lower in the case of no investment in PV, but still interesting.

Finally, economic analysis reveals that, in terms of payback time, the investment considering the installation of the PV system and the alternative bivalent operation is more advantageous in the climatic zone E than in milder climates (zone D), especially compared with the air system. Parallel operation allows a reduction of *DPP* only in cold climates (zones E, F), whereas in zone D there are no appreciable differences. Instead, in terms of *NPW*, the hybrid solution appears more convenient in zone D as it allows for lower CAPEX and annual costs. However, in zones E and F, there is an appreciable increase in *NPW* with a parallel bivalent operation compared with the alternative operation.

As a final remark, it is worth highlighting that, even if not investing in the photovoltaic system allows shorter payback time in colder climates (zones E and F), installation of the PV field makes the hybrid CRT+HP plant proposed here less affected by the variation of the price of grid electricity, which could heavily determine the effective economic viability of this solution.

Author Contributions: Conceptualization, M.N.; methodology, M.N., S.M., F.B. and F.C.; software, M.N. and S.M.; validation, M.N., S.M., F.B. and F.C.; data curation, M.N.; writing—original draft preparation, M.N.; writing—review and editing, M.N., S.M., F.B. and F.C.; supervision, M.N., S.M. and F.C.; project administration, M.N. and S.M.; funding acquisition, M.N. and S.M. All authors have read and agreed to the published version of the manuscript.

Funding: This research project is partially founded by the research agreement "Simulazione dinamica e con metodi computazionali di fluidodinamica di un innovativo sistema ibrido operante con nastri radianti a condensazione e pompa di calore (brevetto domanda n. 102017000136567 depositata il 28/11/2017 e concessa il 13/02/2020) per il condizionamento di edifici industriali" between the University of Padova and Officine Termotecniche Fraccaro s.r.l.

Institutional Review Board Statement: Not applicable.

Informed Consent Statement: Not applicable.

Data Availability Statement: The data that support the findings of this study are available from the corresponding author, M.N., upon reasonable request.

Conflicts of Interest: The authors declare that they have no conflict of interest.

Nomenclature

Symbol	Meaning	Unit
COP	Coefficient of performance	-
f_p	Primary energy factor	-
G	Mass flow rate	[kg s^{-1}]
P	Power	[kW]
PE	Primary energy	[kWh]
PER	Primary energy ratio	-
PES	Primary energy saving	-
QR	Renewable ratio	-
η	Efficiency	-
Subscript	Meaning	
biv	Bivalent	
cond	Condenser	
cut-off	Cut-off	
el	Electricity from the grid	
exp	Electricity exported to the grid	
ext	External	
fuel	Fuel	
heat_source	Heat source of the heat pump (at the evaporator)	
nren	Non-renewable	
out	Outlet	
ren	Renewable	
th	Thermal	
tot	Total	
Acronym	Meaning	Unit
Air	Air heating system	
CFD	Computational fluid dynamics	
CHP	Combined heat and power	
CRF	Condensing radiant floor	
CRT	Condensing radiant tube	
DPP	Discounted payback period	[y]
DSM	Demand side management	
EED	Energy Efficiency Directive	
EU	European Union	
HHV	High heating value	[MJ Sm^{-3}]
HP	Heat pump	
HVAC	Heating, ventilation, air conditioning	
NG	Natural gas	
NPW	Net Present Worth	[€]
PCM	Phase change material	
PV	Photovoltaic	
TES	Thermal energy storage	

References

1. European Commission. Communication from the Commission: A Clean Planet for All. EUR-Lex—52018DC0773—EN—EUR-Lex. 2018. Available online: https://eur-lex.europa.eu/legal-content/en/TXT/?uri=CELEX%3A52018DC0773 (accessed on 2 March 2022).
2. European Union. Directive (EU) 2018/2002 of the European Parliament and of the Council—Of 11 December 2018—Amending Directive 2012/27/EU on Energy Efficiency. 2018. Available online: https://eur-lex.europa.eu/legal-content/EN/TXT/?uri=uriserv%3AOJ.L_.2018.328.01.0210.01.ENG (accessed on 2 March 2022).
3. Malinauskaite, J.; Jouhara, H.; Egilegor, B.; Al-Mansour, F.; Ahmad, L.; Pusnik, M. Energy efficiency in the industrial sector in the EU, Slovenia, and Spain. *Energy* **2020**, *208*, 118398. [CrossRef] [PubMed]
4. Malinauskaite, J.; Jouhara, H.; Ahmad, L.; Milani, M.; Montorsi, L.; Venturelli, M. Energy efficiency in industry: EU and national policies in Italy and the UK. *Energy* **2019**, *172*, 255–269. [CrossRef]
5. Muriel de Oliveira, G. Research and Development Financing in the Renewable Energy Industry in Brazil. *J. Sustain. Dev. Energy Water Environ. Syst.* **2014**, *2*, 208–218. [CrossRef]

6. Leobner, I.; Smolek, P.; Heinzl, B.; Raich, P.; Schirrer, A.; Kozek, M.; Rössler, M.; Mörzinger, B. Simulation-based Strategies for Smart Demand Response. *J. Sustain. Dev. Energy Water Environ. Syst.* **2018**, *6*, 33–46. [CrossRef]
7. Paulus, M.; Borggrefe, F. The potential of demand-side management in energy-intensive industries for electricity markets in Germany. *Appl. Energy* **2011**, *88*, 432–441. [CrossRef]
8. Mikulčić, H.; Vujanović, M.; Duić, N. Reducing the CO_2 emissions in Croatian cement industry. *Appl. Energy* **2013**, *101*, 41–48. [CrossRef]
9. López Pérez, S.; Herrero López, S.; Ubieta Astigarraga, E.; del Hoyo Arce, I.; Gómez de Arteche Botas, M.; Iturralde Iñarga, J.; Fernández de Arroiabe Txapartegi, P.; Mounir Bou-Ali, M.; Unamuno Iriondo, I. Design of a Radiant Heat Capturing Device for Steel Mills. *J. Sustain. Dev. Energy Water Environ. Syst.* **2021**, *9*, 1080365. [CrossRef]
10. Alshehhi, I.; Alnahdi, W.; Ali, M.; Bouabid, A.; Sleptchenko, A. Assessment of Waste Heat Recovery in the Steel Industry. *J. Sustain. Dev. Energy Water Environ. Syst.* **2023**, *11*, 1100440. [CrossRef]
11. Lazzarin, R.; Noro, M. Energy efficiency opportunities in the service plants of cast iron foundries in Italy. *Int. J. Low Carbon Technol.* **2017**, *12*, 96–109. [CrossRef]
12. Lazzarin, R.; Noro, M. Energy efficiency opportunities in the production process of cast iron foundries: An experience in Italy. *Appl. Therm. Eng.* **2015**, *90*, 509–520. [CrossRef]
13. López-Sabirón, A.M.; Royo, P.; Ferreira, V.J.; Aranda-Usón, A.; Ferreira, G. Carbon footprint of a thermal energy storage system using phase change materials for industrial energy recovery to reduce the fossil fuel consumption. *Appl. Energy* **2014**, *135*, 616–624. [CrossRef]
14. Righetti, G.; Lazzarin, R.; Noro, M.; Mancin, S. Phase Change Materials embedded in porous matrices for hybrid thermal energy storages: Experimental results and modelling. *Int. J. Refrig.* **2019**, *106*, 266–277. [CrossRef]
15. Lazzarin, R.; Mancin, S.; Noro, M.; Righetti, G. Hybrid PCM—Aluminium foams' thermal storages: An experimental study. *Int. J. Low Carbon Technol.* **2018**, *13*, 286–291. [CrossRef]
16. Gambini, M.; Vellini, M.; Stilo, T.; Manno, M.; Bellocchi, S. High-Efficiency Cogeneration Systems: The Case of the Paper Industry in Italy. *Energies* **2019**, *12*, 335. [CrossRef]
17. Vialetto, G.; Noro, M.; Colbertaldo, P.; Rokni, M. Enhancement of energy generation efficiency in industrial facilities by SOFC—SOEC systems with additional hydrogen production. *Int. J. Hydrog. Energy* **2019**, *44*, 9608–9620. [CrossRef]
18. Vialetto, G.; Noro, M. An innovative approach to design cogeneration systems based on big data analysis and use of clustering methods. *Energy Convers. Manag.* **2020**, *214*, 112901. [CrossRef]
19. Vialetto, G.; Noro, M. Enhancement of a Short-Term Forecasting Method Based on Clustering and kNN: Application to an Industrial Facility Powered by a Cogenerator. *Energies* **2019**, *12*, 4407. [CrossRef]
20. Schützenhofer, S.; Kovacic, I.; Rechberger, H. Assessment of sustainable use of material resources in the Architecture, Engineering and Construction industry—A conceptual Framework proposal for Austria. *J. Sustain. Dev. Energy Water Environ. Syst.* **2022**, *10*, 1100417. [CrossRef]
21. European Union. Directive (EU) 2018/844 of the European Parliament and of the Council of 30 May 2018 Amending Directive 2010/31/EU on the Energy Performance of Buildings and Directive 2012/27/EU on Energy Efficiency. Available online: https://eur-lex.europa.eu/legal-content/EN/TXT/PDF/?uri=CELEX:32018L0844&from=IT (accessed on 2 March 2022).
22. Trianni, A.; Cagno, E.; De Donatis, A. A framework to characterize energy efficiency measures. *Appl. Energy* **2014**, *118*, 207–220. [CrossRef]
23. Katunska, J.; Oberleova, J.; Rusnak, A.; Toth, S. Diagnosis of elected industrial hall object and idea for its reconstruction. *Adv. Mater. Res.* **2014**, *1057*, 19–26. [CrossRef]
24. Chinese, D.; Nardin, G.; Saro, O. Multi-criteria analysis for the selection of space heating systems in an industrial building. *Energy* **2011**, *36*, 556–565. [CrossRef]
25. Caputo, A.C.; Pelagagge, P.M. Upgrading mixed ventilation systems in industrial conditioning. *Appl. Therm. Eng.* **2009**, *29*, 3204–3211. [CrossRef]
26. Gourlis, G.; Kovacic, I. A study on building performance analysis for energy retrofit of existing industrial facilities. *Appl. Energy* **2016**, *184*, 1389–1399. [CrossRef]
27. Gourlis, G.; Kovacic, I. Passive measures for preventing summer overheating in industrial buildings under consideration of varying manufacturing process loads. *Energy* **2017**, *137*, 1175–1185. [CrossRef]
28. Kovacic, I.; Waltenbereger, L.; Gourlis, G. Tool for life cycle analysis of facade-systems for industrial buildings. *J. Clean. Prod.* **2016**, *130*, 260–272. [CrossRef]
29. Smolek, P.; Leobner, I.; Gourlis, G.; Mörzinger, B.; Heinzl, B.; Ponweiser, K. Hybrid Building Performance Simulation Models for Industrial Energy Efficiency Applications. *J. Sustain. Dev. Energy Water Environ. Syst.* **2018**, *6*, 381–393. [CrossRef]
30. Gourlis, G.; Kovacic, I. Building Information Modelling for analysis of energy efficient industrial buildings—A case study. *Renew. Sustain. Energy Rev.* **2017**, *68*, 953–963. [CrossRef]
31. Stamponi, E.; Lattanzi, N.; Moretti, E. Experimental and numerical assessment for HVAC management in an industrial building: A preliminary optimization. *J. Phys. Conf. Ser.* **2021**, *2069*, 012111. [CrossRef]
32. Selim, O.M.; Abousabae, M.; Hasan, A.; Amano, R.S. Analysis of energy savings and CO_2 emission reduction contribution for industrial facilities in USA. *J. Energy Resour. Technol. Trans. ASME* **2021**, *143*, 082303. [CrossRef]
33. Lazzarin, R. *Interview on Space Heating in Industry*; SGE: Padova, Italy, 2002. (In Italian)

34. Brunello, P.; De Carli, M.; Magagnin, P.; Polito, A.; Zecchin, R. Gas radiant heating in industrial environments: Phenomenology, design, verification. In Proceedings of the AiCARR Congress “Progettare L'involucro Edilizio: Correlazioni Tra il Sistema Edificio e i Sistemi Impiantistici”, Bologna, Italy, 18 October 2001; pp. 183–204. (In Italian).
35. De Carli, M.; Polito, A. Radiant air conditioning systems. In Proceedings of the AiCARR Congress “Riduzione dei Fabbisogni, Recupero di Efficienza e Fonti Rinnovabili per il Risparmio Energetico Nel Settore Industriale”, Padova, Italy, 17 June 2010; pp. 43–80. (In Italian).
36. Brunello, P.; De Carli, M.; Polito, A.; Zecchin, R. Comfort criteria and design aspects in high temperature radiant heating. In Proceedings of the Indoor Air 2002, Monterey, CA, USA, 30 June–5 July 2002.
37. D'Ambrosio Alfano, F.R. The thermal environment in industry. In Proceedings of the AiCARR Congress “Riduzione dei Fabbisogni, Recupero di Efficienza e Fonti Rinnovabili per il Risparmio Energetico Nel Settore Industriale”, Padova, Italy, 17 June 2010; pp. 11–30. (In Italian).
38. Lazzarin, R. *Condensing Boilers*; PEG: Milano, Italy, 1986. (In Italian)
39. Noro, M.; Lazzarin, R. Energy analysis of industrial climatization by an innovative radiant condensing system. *AIP Conf. Proc.* **2019**, *2191*, 020121. [CrossRef]
40. Noro, M.; Mancin, S.; Cerboni, F. High efficiency hybrid radiant and heat pump heating plants for industrial buildings: An energy analysis. *Int. J. Heat Technol.* **2022**, *40*, 863–870. [CrossRef]
41. Italian Government. DECRETO LEGISLATIVO 3 Marzo 2011, n. 28 Attuazione Della Direttiva 2009/28/CE Sulla Promozione Dell'uso Dell'energia da Fonti Rinnovabili, Recante Modifica e Successiva Abrogazione Delle Direttive 2001/77/CE e 2003/30/CE. (In Italian). Available online: https://www.gazzettaufficiale.it/eli/gu/2011/03/28/71/so/81/sg/pdf (accessed on 2 March 2022).
42. Italian Economic Development Ministry. Decreto Interministeriale 26 Giugno 2015—Adeguamento Linee Guida Nazionali per la Certificazione Energetica Degli Edifici. (In Italian). Available online: https://www.mise.gov.it/index.php/it/normativa/decreti-interministeriali/decreto-interministeriale-26-giugno-2015-adeguamento-linee-guida-nazionali-per-la-certificazione-energetica-degli-edifici?fbclid=IwAR0b1hSl5RfM4gkwQl14MuTMPZTjoaQcbJc5TDupjldOBSihzHZsfJiILyM?hitcount=0?hitcount=0?hitcount=0?hitcount=0?hitcount=0?hitcount=0?hitcount=0?hitcount=0?hitcount=0?hitcount=0?hitcount=0?hitcount=0 (accessed on 2 March 2022).
43. *UNI/TS 11300-5:2016*; Prestazioni Energetiche Degli Edifici—Parte 5: Calcolo Dell'energia Primaria e Della Quota di Energia da Fonti Rinnovabili. Italian Standard Organization: Milano, Italy, 2016. (In Italian)
44. Italian Government. DECRETO LEGISLATIVO 8 Novembre 2021, n. 199 Attuazione della Direttiva (UE) 2018/2001 del Parlamento Europeo e del Consiglio, dell'11 dicembre 2018, Sulla Promozione Dell'uso Dell'energia da Fonti Rinnovabili. (In Italian). Available online: https://www.gazzettaufficiale.it/eli/id/2021/11/30/21G00214/sg (accessed on 2 March 2022).
45. Italian Government. Decreto del Presidente Della Repubblica 26 Agosto 1993, n. 412 Regolamento Recante Norme per la Progettazione, L'installazione, L'esercizio e la Manutenzione Degli Impianti Termici Degli Edifici ai Fini del Contenimento dei Consumi di Energia, in Attuazione Dell'art. 4, Comma 4, Della Legge 9 Gennaio 1991, n. 10. (In Italian). Available online: https://www.gazzettaufficiale.it/eli/id/1993/10/14/093G0451/sg (accessed on 2 March 2022).
46. CTI—Comitato Termotecnico Italiano. Weather Reference Year. (In Italian). Available online: https://www.cti2000.it/index.php?controller=news&action=show&newsid=34985 (accessed on 15 July 2021).
47. ENE. Azioni Amministrative e Comportamentali per la Riduzione del Fabbisogno Nazionale di Gas Metano. Settore Residenziale. 2022. Available online: https://www.enea.it/it/seguici/events/conferenza-stampa/RapportotecnicoAzioniperlariduzionedel-FabbisognoNazionalediGas.pdf (accessed on 30 January 2023).
48. Fraunhofer Institute for Solar Energy Systems. Photovoltaics Report. 2021. Available online: https://www.ise.fraunhofer.de/content/dam/ise/de/documents/publications/studies/Photovoltaics-Report.pdf (accessed on 1 September 2022).